Ulnomeniscal Homologue of the Wrist: Correlation of Anatomic and MR Imaging Findings[1]

Florian M. Buck, MD
Ramon Gheno, MD
Marcelo A. C. Nico, MD
Parviz Haghighi, MD
Debra J. Trudell
Donald Resnick, MD

Purpose: To evaluate the anatomy of the ulnar side of the wrist in the region of the triangular fibrocartilage (TFC) complex, with special focus on the ulnomeniscal homologue (UMH) and its relationship to surrounding structures.

Materials and Methods: Institutional review board approval and informed consent were not required. Ten upper extremities were harvested from the nonembalmed cadavers of four women and six men (age range at death, 56–97 years; mean age at death, 83 years) and used according to institutional guidelines. Magnetic resonance (MR) imaging and MR arthrography of the wrist were performed with the wrist in neutral position, maximal ulnar deviation, and maximal radial deviation by using intermediate-weighted sequences. The specimens were cut into 4-mm-thick sections that corresponded to the MR imaging planes. The gross anatomic features of the UMH and its relationship to adjacent structures were evaluated and compared with imaging findings. UMH variants, as described in previous articles on purely anatomic studies, were sought on MR images. MR findings of the wrist in neutral position were compared with those of the wrist in maximal ulnar and radial deviations. Histologic examination was used to further elucidate the structure of the UMH.

Results: The UMH displayed complex anatomic features because of its obliquely oriented course. However, it could be divided into styloid, radioulnar, and collateral components and a distal insertion. The UMH variants described in previously published studies could be identified, but evaluation results were highly dependent on the wrist position at imaging.

Conclusion: The anatomy of the UMH is complex. For assessment of the UMH and the ulnar side of the TFC complex, coronal MR arthrography with the wrist in neutral position or radial deviation might be superior to standard MR imaging.

[1] From the Departments of Radiology (F.M.B., R.G., M.A.C.N., D.J.T., D.R.) and Pathology (P.H.), Veterans Affairs San Diego Healthcare System, San Diego, Calif. Received April 29, 2009; revision requested June 2; revision received June 5; accepted June 25; final version accepted June 27. Supported by the Swiss National Science Foundation and the Swiss Radiological Society. **Address correspondence to** F.M.B., Department of Radiology, Orthopedic University Hospital Balgrist, Forchstrasse 340, CH-8008 Zurich, Switzerland.

The ulnomeniscal homologue (UMH) of the wrist was first described in 1970 by Lewis et al (1). It is located centrally at the ulnar aspect of the radiocarpal joint, adjacent to the triangular fibrocartilage (TFC), radioulnar and ulnocarpal ligaments, styloid process of the ulna, prestyloid recess of the radiocarpal joint, sheath of the extensor carpi ulnaris (ECU) tendon, and ulnar collateral ligament. A great deal has been written about the anatomy and injury patterns of the TFC complex and the ulnar side of the wrist (2–14). The UMH has been mentioned in only a few articles, however, and some controversy about the anatomy and different anatomic variants of this region remains.

Abnormalities of the UMH might be a cause of ulnar-side wrist pain. On the basis of arthroscopic and anatomic specimen findings, Nishikawa et al (15) described an ulnar detachment injury of the UMH. However, this injury has not yet been documented with magnetic resonance (MR) imaging or MR arthrography. In our experience, this lesion is occult at standard MR imaging but might be detected with MR arthrography. In addition, the diagnosis of distal avulsion injuries of the TFC complex according to the classification system of Palmer (16) remains difficult because of the complex anatomy and limited spatial resolution of MR images. Knowledge about the anatomy, anatomic variants, and MR imaging characteristics of the UMH is a likely prerequisite for accurate diagnosis of pathologic changes, such as trauma and degeneration. Thus, the purpose of this study was to evaluate the anatomy of the ulnar side of the wrist in the region of the TFC complex, with a special focus on the UMH and its relationship to surrounding structures to acquire further clues to the diagnosis of UMH lesions.

Advances in Knowledge

- We describe the anatomic and histologic features of the ulnomeniscal homologue (UMH) and its imaging characteristics in a correlative MR imaging–anatomic study.
- The anatomic variants of the UMH described in previously published studies can be identified on MR images, on which their appearance depends on the position of the wrist at the time of image acquisition.

Materials and Methods

Specimens

Institutional review board approval and informed consent were not required. Ten upper extremities were harvested from the nonembalmed cadavers (age range at death, 56–97 years; mean age at death, 83 years) of four women (age range at death, 85–97 years; mean age at death, 90 years) and six men (age range at death, 56–90 years; mean age at death, 78 years). The specimens included the entire hand, forearm, elbow, and distal portion of the humerus. Immediately after being harvested, all of the specimens were deep frozen at −40°C (Forma Bio-Freezer; Forma Scientific, Marietta, Ohio) and then allowed to thaw for 24 hours at room temperature before MR imaging.

MR Imaging

MR images were acquired with a 1.5-T MR system (Signa; GE Medical Systems, Milwaukee, Wis). A dedicated receive-only wrist coil was used. The specimens were imaged in three distinct positions: Specimens were imaged with the wrist in neutral position with the palm down, longitudinal to the gantry. The elbow was flexed 90° to ensure correct positioning in the neutral position, without pronation or supination of the forearm. The specimens were also imaged in the same neutral position but in both maximal ulnar and maximal radial deviations of the radiocarpal joint. To ensure maximal radial and ulnar deviations, the wrist was fixed within the wrist coil with a piece of tape and gentle tension was applied to the fingers by using another piece of tape.

Non–fat-saturated and fat-saturated intermediate-weighted fast spin-echo sequences (3000/32 [repetition time msec/echo time msec]; matrix, 512 × 512; field of view, 7 × 7 cm; section thickness, 2 mm; number of acquired signals, two; echo train length, six; bandwidth, ±31 kHz) were acquired in the transverse, sagittal, and coronal planes.

MR Arthrography and Tenography

Contrast medium was injected in a standardized fashion into the distal radioulnar joint, radiocarpal joint, midcarpal joint, and sheath about the ECU tendon by a fellowship-trained musculoskeletal radiologist (M.A.C.N.) with 4 years of experience in arthrography. After fluoroscopic confirmation of the intraarticular position of the tip of the needle, 2 mL of gadopentetate dimeglumine (Magnevist; Bayer-Schering, Berlin, Germany) diluted in 250 mL of saline and mixed with an equal amount of iodinated contrast agent (iohexol, Omnipaque 350; Bayer Healthcare Pharmaceuticals, Leverkusen, Germany) was injected. The injection volumes were 2 mL for the distal radioulnar joint and 3 mL for the radiocarpal joint and midcarpal joints.

Tenography was performed with ultrasonographic guidance (iU22 Ultrasound System, C12-5 linear array transducer; Philips Medical Systems, Best, the Netherlands). The tip of the needle was placed proximal to the base of the ulnar styloid process between the ECU tendon and the ECU

Published online before print
10.1148/radiol.2533090743

Radiology 2009; 253:771–779

Abbreviations:
ECU = extensor carpi ulnaris
TFC = triangular fibrocartilage
UMH = ulnomeniscal homologue

Author contributions:
Guarantors of integrity of entire study, F.M.B., M.A.C.N., D.R.; study concepts/study design or data acquisition or data analysis/interpretation, all authors; manuscript drafting or manuscript revision for important intellectual content, all authors; manuscript final version approval, all authors; literature research, F.M.B., M.A.C.N., D.R.; experimental studies, F.M.B., R.G., P.H., D.J.T.; statistical analysis, F.M.B.; and manuscript editing, F.M.B., D.R.

Authors stated no financial relationship to disclose.

tendon sheath. Passage of the injected contrast media in a linear fashion along the tendon confirmed the correct position of the needle tip. The injection volume was 4 mL, with the same mixture of iodinated and MR contrast media that was used for arthrography. After arthrography and tenography, the intermediate-weighted fast spin-echo MR sequences were repeated with the wrist in neutral position and in ulnar and radial deviations.

Preparation of Anatomic Sections

After imaging, a band saw was used to divide the specimens into 3–4-mm-thick sections that corresponded to the imaging planes used for MR imaging. Three specimens were sectioned in the transverse plane in the neutral position, six specimens were sectioned in the coronal plane (four in neutral position, one in ulnar deviation, and one in radial deviation), and one specimen was sectioned in the sagittal plane in neutral position. Conventional radiographs and photographs of each section were obtained.

Image Analysis

The photographs of the anatomic sections were compared with the MR images by two fellowship-trained musculoskeletal radiologists (F.M.B., R.G., both with 4 years of experience in musculoskeletal radiology) in consensus. The UMH was identified, and its borders and relationships to adjacent structures (ulnar styloid process, radioulnar ligaments, TFC, prestyloid recess, ulnar collateral ligament) were noted. The type of UMH with respect to the prestyloid recess was determined according to the criteria of Ishii et al (7). All anatomic findings were then evaluated on the MR arthrographic images.

Histologic Assessment

Five tissue samples were taken from the different parts of the UMH. The samples were then fixed in 10% neutral buffered formalin for at least 72 hours, decalcified, and embedded in paraffin wax. After being cut into 4-μm sections with a sliding microtome, the tissue was mounted onto slides and stained with hematoxylin-eosin. The histologic architecture of all parts of the UMH and the regions of transition between the UMH and the adjacent structures were evaluated by a skeletal pathologist (P.H.) with 30 years of experience.

Results

At gross examination, the UMH was identified as a white fibrous structure. Proximally, it was bordered by the TFC, ulnar styloid process, and distal lamina of the dorsal and ventral radioulnar ligaments. On the ulnar side, it was bordered by the ulnar styloid process, ECU tendon sheath, and ulnar-side joint capsule of the radiocarpal joint. Distally, the UMH abutted the ulnar aspect of the triquetrum.

In addition, some fibers extended more distally to reach the ulnar aspect of the hamate bone and the base of the fifth metacarpal bone, where they merged with the ulnar collateral ligament. The latter ligament was appreciated only as a subtle thickening of the capsule of the radiocarpal joint.

The UMH could be divided into styloid, radioulnar, and collateral components and a distal insertion (Fig 1). The principal part (ie, root portion) of the UMH was the styloid component, whereas the other three components could be viewed as extensions of this component. They served as a suspension of the UMH to the surrounding structures.

Radioulnar Component

The radioulnar component of the UMH arose at the dorsal edge of the radial notch, together with the dorsal radioulnar ligament of the TFC complex. The fibers of the radioulnar component coursed in an ulnar orientation, dorsally, and distally to the dorsal radioulnar ligament; deep to the radiotriquetral and ulnotriquetral ligaments; and around the ulnar aspect of the triquetrum to the tip of the styloid process of the ulna (Figs 2, 3). The radioulnar component merged with the styloid component posteriorly and distally to the opening to the prestyloid recess.

Histologically, the radioulnar component of the UMH consisted of densely packed collagen fibers that were indistinguishable proximally from the dorsal radioulnar ligament. Visualization of this component was difficult on MR images. The most useful images were obtained in

Figure 1

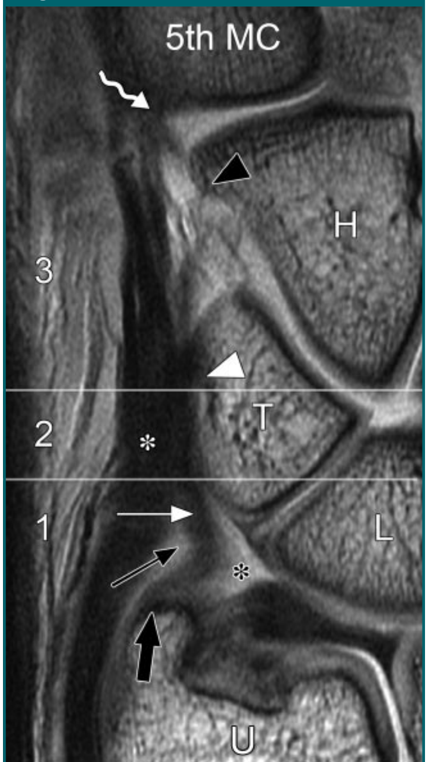

Figure 1: Coronal intermediate-weighted MR image of the UMH at the level of the tip of the ulnar styloid process (thick black arrow). The styloid component (region *1*), collateral component (region *2*), and distal insertion (region *3*) are visible (separated with horizontal lines). The styloid component is recognized between the entrance to the prestyloid recess (black asterisk) and the ECU tendon (white asterisk). It can be divided into a more fibrous part (straight white arrow) and a highly vascular part with interspersed fat tissue (thin black arrow). Next to the prestyloid recess, the styloid component attaches to the ulnar styloid process. At the level of the collateral component, there is no high signal intensity (highly vascular tissue) between the ECU tendon and the UMH. The main part of the distal insertion attaches to the ulnar aspect of the triquetrum (*T*, white arrowhead). It also attaches to the hamate bone (*H*, black arrowhead) and the fifth metacarpal bone (*5th MC*, wavy arrow). *L* = lunate bone, *U* = ulna.

the sagittal plane (Fig 2). Arthrography or at least a small joint effusion was required to identify this part of the UMH.

Styloid Component

The styloid component formed the main body of the UMH, was located distal to the TFC (between the tip of the styloid process and the ulnar aspect of the triquetrum), and surrounded the entrance to the prestyloid recess of the radiocarpal joint (Fig 4). In the coronal plane, this component had a typical triangular shape, with the base of the triangle located along the ECU tendon sheath. At histologic evaluation, it was shown to consist of two distinct parts: The base of the triangle was composed of highly vascular connective tissue with irregularly oriented collagen fibers (Fig 5). The radial aspect of the styloid component consisted of densely packed collagen fibers uniformly oriented in the proximal-distal direction, similar to a seatbelt extending around the triquetrum in a proximal-distal–to-distal volar direction. In the transverse plane, the styloid component was ovoid and located between the ECU tendon sheath, the TFC, and the ulnar aspect of the triquetrum on the radial side (Fig 6). The styloid component was broadly attached to the TFC and the ECU tendon sheath. Histologic evaluation showed no border between the ECU tendon sheath and the UMH; rather, continuous collagen fibers connected both structures (Fig 5). In addition, the styloid component was held in place by a small attachment slightly volar to the tip of the ulnar styloid process, adjacent to the prestyloid recess. This component was best seen on coronal MR images. Its heterogeneous histologic composition was reflected as high signal intensity at the base of the triangle adjacent to the ECU tendon (Fig 1).

The entrance to the prestyloid recess was seen as a small aperture in the styloid portion that widened to form a small channel that enlarged to become the prestyloid recess at the anterior aspect of the ulnar styloid process. All three types of UMH, as defined by Ishii et al (7), could be identified. Five specimens had a narrow opening (Fig 7), three had a wide opening (Fig 8), and two had no apparent opening (Fig 9). On the MR images obtained before arthrography, the prestyloid recess in four specimens was col-

Figure 2

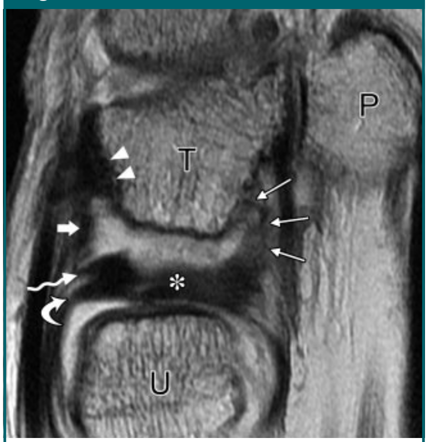

Figure 2: Sagittal intermediate-weighted MR image shows anatomic features of the UMH slightly ulnar to the origin of the dorsal radioulnar ligament (curved arrow) and radioulnar component (wavy arrow) of the UMH. The radioulnar component extends to the distal contour of the dorsal radioulnar ligament. The TFC is marked with an asterisk. The ulnotriquetral ligament is noted as a thickening of the dorsal joint capsule (thick arrow). The insertion of the radiotriquetral ligament (arrowheads) is seen in the dorsal aspect of the triquetrum *(T).* On the volar side, the distal insertion of the UMH is seen with its main body (thin straight arrows) attaching to the triquetrum. *P* = pisiform, *U* = ulna.

Figure 3

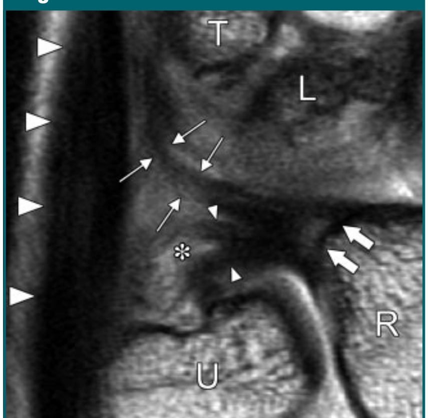

Figure 3: Coronal intermediate-weighted MR image shows radioulnar component (thin arrows) of the UMH at the level of the origin of the dorsal radioulnar ligament. The broad ligamentous structure attaches to the dorsal edge of the radial notch (thick arrows) and divides into the proximal and distal lamina of the TFC (small arrowheads), separated by the ligamentum subcruentum (*), and the radioulnar component. Large arrowheads point to ECU tendon. *L* = lunate bone, *R* = radius, *T* = triquetrum, *U* = ulna.

Figure 4

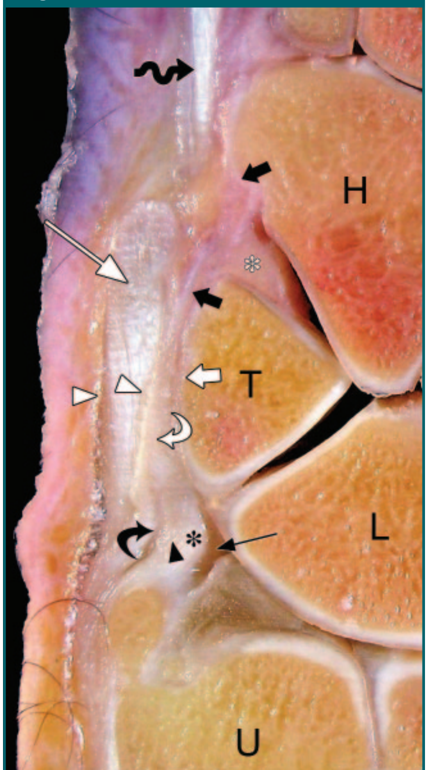

Figure 4: Gross specimen shows anatomic features of the UMH in the coronal plane at the level of the tip of the ulnar styloid process. The styloid component of the UMH is seen at the tip of the ulnar styloid process. It is composed of a white ligamentous part (black asterisk) on the radial side and a more fatty, slightly yellow part (black arrowhead) next to the ulnar collateral ligament and the ECU tendon sheath (curved black arrow). The entrance to the prestyloid recess (long straight black arrow) lies between the UMH and the TFC. The opening to the prestyloid recess is the narrow type. More distally, the collateral part of the UMH, the ECU tendon sheath, and the ulnar collateral ligament merge into one structure (curved white arrow). The UMH attaches distally to the ulnar aspect of the triquetrum (*T,* short white arrow) and to the ulnar facet of the hamate bone (*H,* short black arrows), where it fuses with the joint capsule and a meniscus-shaped fatty fringe (white asterisk) between the hamate bone and the triquetrum. Wavy black arrow points to extensor digiti minimi tendon, long white arrow points to ECU tendon, white arrowheads also point to ECU tendon sheath. *L* = lunate bone, *U* = ulna.

lapsed. The opening could not be identified on these images and thus led to the potential misdiagnosis of UMH type with no opening.

For all specimens, MR arthrography enabled differentiation between the type that has no opening and the type that has a wide or narrow opening (Table). The best imaging plane for this differentiation was the coronal plane, but the type of entrance could also be identified in the transverse plane in five specimens and in the sagittal plane in one specimen. Because of the distention of the joint space by contrast media, however, it was difficult to ascertain whether the opening was wide or narrow.

In addition, the apparent width of the opening was heavily dependent on the imaging position (Table). In maximal ulnar deviation, the entrance to the prestyloid recess was collapsed, simulating the no-opening type, on the MR images of all specimens and on the MR arthrographic images of four specimens. In maximal radial deviation, narrow-opening and wide-opening types became far more evident (Figs 7, 8).

Collateral Component

The collateral component of the UMH was the short distal extension of the styloid component along the ECU tendon sheath (Figs 1, 4). On the ulnar side, it was completely fused with the ECU tendon sheath dorsally and fused with the slightly thick region of the joint capsule attributed to the ulnar collateral ligament ventrally.

Histologic assessment revealed no border between the collateral component of the UMH, the ECU tendon sheath, and the joint capsule (Fig 5). However, there were clear fibers from the UMH that merged with these structures to form a strong fibrous cord that extended from the tip of the ulnar styloid process of the ulna to the insertion of the UMH at the ulnar aspect of the triquetrum. This component was best seen on coronal and transverse MR images (Fig 1).

Distal Insertion

The distal component of the UMH was evident at the caudal end of the collateral component (Fig 1). Four distinct insertion sites were identified: ulnar aspect of the triquetrum, ulnar aspect of the hamate bone, base of the fifth metacarpal bone, and dorsal capsular ligament of the pisotriquetral joint. The ulnar aspect of the triquetrum represented the main insertion site and was clearly visible in all specimens. This insertion consisted of a broad fibrous strand that attached to the triquetrum, together with the ulnar collateral ligament. There was some variability in the width of this attachment, as described by Hogikyan and Louis (9) and as shown in the Table.

The insertions in the ulnar aspect of the hamate bone and the ulnar side of the base of the fifth metacarpal bone were visible only as thin fibrous strands (Figs 1, 4). The fibers attaching to the hamate bone formed two fine strands inserting at two distinct locations into the ulnar aspect of the hamate bone. One of these strands inserted into the most ulnar tip of the bone, and the other inserted at a slightly more volar orientation into a small groove adjacent to the insertion of

Figure 5

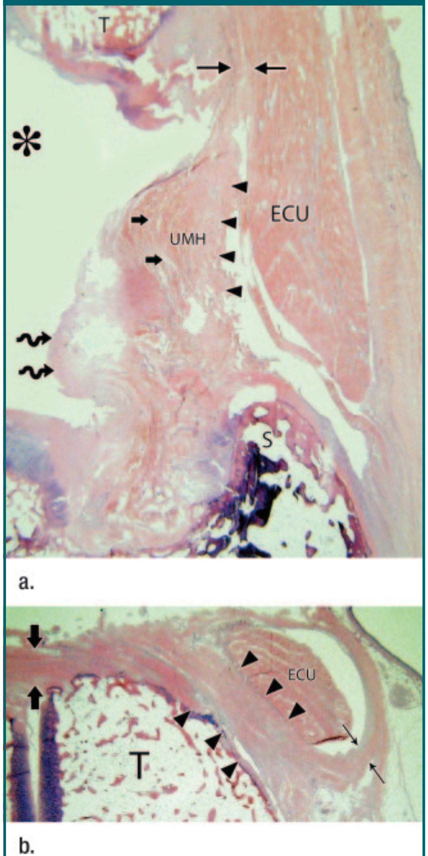

Figure 5: Hematoxylin-eosin–stained histologic sections of the UMH. (Magnification, ×2.) **(a)** In the coronal plane, the styloid component of the UMH is seen as a triangular structure. The base of the triangle is composed of highly vascular, friable connective tissue (arrowheads) with irregular collagen fibers. The radial aspect consists of densely packed collagen fibers (thick arrows). More distally, the UMH, ECU tendon sheath, ulnar collateral ligament, and joint capsule merge to form one structure (thin arrows) composed of densely packed collagen fibers. The lunate bone was removed (*). The TFC (wavy arrows) is torn distally. *S* = styloid process of the ulna. **(b)** In the transverse plane, the distal UMH is seen between the ulnar aspect of the triquetrum *(T)* and the ECU tendon (arrowheads). The joint capsule, ulnar collateral ligament, and ECU tendon sheath (thin arrows) are indistinguishable from the UMH. The ECU tendon sheath is seen only at the volar aspect of the ECU tendon. The dorsal part of the lunotriquetral ligament (thick arrows) is also evident.

Figure 6

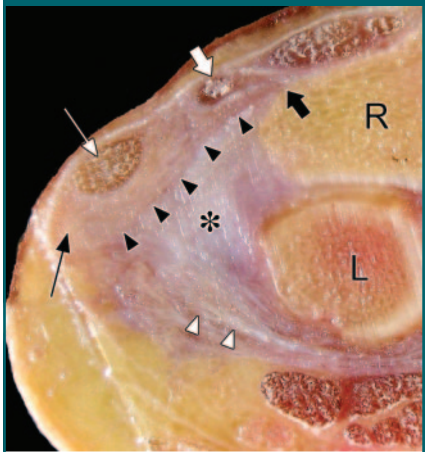

Figure 6: Gross specimen shows anatomic features of the UMH in the transverse plane at the level of the TFC (*), slightly distal to the tip of the ulnar styloid process. The UMH inserts at the dorsal edge of the radial notch (thick black arrow) of the radius *(R)*, together with the dorsal radioulnar ligament. It courses volar to the extensor digiti minimi tendon (thick white arrow) and ECU tendon (thin white arrow) to the tip of the ulnar styloid process. The border (black arrowheads) between the TFC and the UMH is well shown. The UMH is indistinguishable from the ulnar collateral ligament (thin black arrow) and the ECU tendon sheath. The volar radioulnar ligament (white arrowheads) is partially seen. The lunate bone *(L)* is partially truncated.

the joint capsule (Fig 4). The latter was often intertwined with a meniscus-shaped fat fringe that reached between the distal triquetrum and the hamate bone.

Some fibers ran a more volar course and combined with a delicate fibrous strand that arose from the volar aspect of the ECU tendon sheath and reached the ulnar aspect of the pisiform, contributing to the dorsal capsular ligament of the pisotriquetral joint (17) (Fig 10). The entire distal insertion was clearly separated

Figure 7

a. b. c.

Figure 7: Narrow-opening UMH type with respect to the entrance to the prestyloid recess. **(a)** Anatomic section and **(b, c)** intermediate-weighted MR images obtained with the wrist in neutral position (**b**) and maximal radial deviation (**c**) are shown. *T* = triquetrum, *U* = ulna. **(a)** The styloid component of the UMH is recognized as white fibrous tissue (arrowheads). *L* = lunate bone. The entrance to the prestyloid recess (wavy arrow) is well seen. The entrance is clearly wider in **c**, mimicking the wide-opening type.

Figure 8

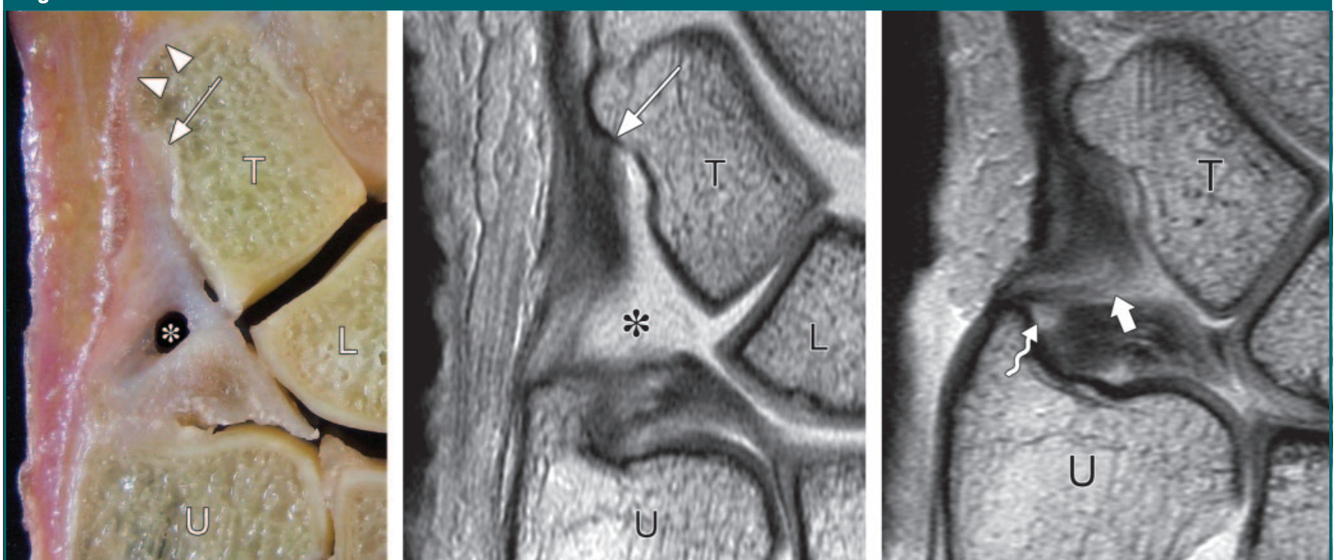

a. b. c.

Figure 8: Wide-opening UMH type with respect to the entrance to the prestyloid recess. **(a)** Anatomic section and **(b, c)** intermediate-weighted MR images obtained with the wrist in neutral position (**b**) and maximal ulnar deviation (**c**) are shown. *T* = triquetrum, *U* = ulna. In **a** and **b**, the entrance (asterisk) to the prestyloid recess is well shown. *L* = lunate bone. In **b**, the entrance seems to be wider, probably because of its distention after injection of the contrast agent. In **c**, the entrance (straight arrow) to the prestyloid recess is almost totally collapsed; the recess is partially visible at the tip of the ulnar styloid process (wavy arrow). In addition, the distal insertion of the UMH (thin arrow in **a** and **b**) is well shown at the ulnar aspect of the triquetrum. The fibers inserting into the ulnar aspect of the hamate bone extend around the distal triquetrum (arrowheads in **a**). A complete tear of the lunotriquetral ligament is also seen.

Radiology

Figure 9

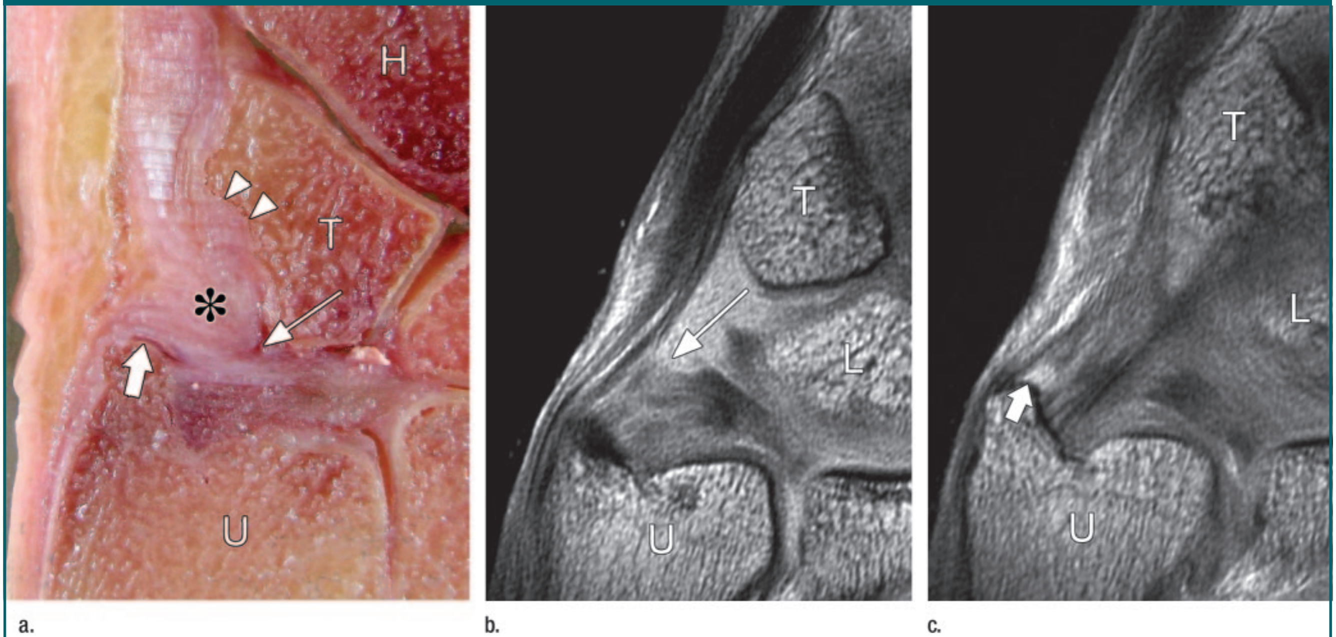

Figure 9: No-opening UMH type with respect to the entrance to the prestyloid recess. **(a)** Anatomic section and **(b, c)** intermediate-weighted MR images obtained with the wrist in maximal radial deviation are shown. *T* = triquetrum, *U* = ulna. In **a**, there is no communication between the small prestyloid recess (thick arrow) and the radiocarpal joint space (thin arrow), and the UMH (*) is relatively large and has a broad attachment (arrowheads) to the ulnar aspect of the triquetrum. *H* = hamate bone. In **b** and **c**, there is also no communication between the radiocarpal joint space (thin arrow in **b**) and the small prestyloid recess (thick arrow in **c**) at the tip of the ulnar styloid process. *L* = lunate bone.

from the volar extrinsic ligaments (volar ulnotriquetral and volar ulnolunate ligaments) that lay more on the ulnar aspect of the triquetrum.

The insertion in the triquetrum was always seen on the coronal MR images. The other insertions were seen only in six specimens, and the fibers of the ulnar collateral ligament and the insertion in the hamate bone and the fifth metacarpal bone were barely distinguishable. In accordance with the work of Nishikawa and Toh (8), we found some variability in the distal insertions of the UMH (Table). The different types of insertions were best seen on the coronal images obtained with the wrist in neutral position. Bicompartmentalization of the radiocarpal joint was not evident in our specimens.

Evaluation of UMH Subtypes Based on Criteria Used in Previously Published Studies

Specimen No.	Prestyloid Recess Opening at MR Arthrography*			Distal Insertion Type[†]	Attachment Type[‡]
	Neutral Position	Ulnar Deviation	Radial Deviation		
1	Narrow	Narrow	Wide	1	1
2	Narrow	No opening	Narrow	2	2
3	No opening	No opening	No opening	2	2
4	No opening	No opening	No opening	1	2
5	Wide	Narrow	Wide	1	1
6	Wide	No opening	Wide	1	1
7	Wide	Narrow	Wide	2	1
8	Narrow	Narrow	Wide	1	1
9	Narrow	No opening	Wide	2	3
10	Narrow	No opening	Narrow	2	3

* Prestyloid recess openings were defined on the basis of the criteria of Ishii et al (7).

[†] Distal insertion types are based on the criteria used by Nishikawa and Toh (8): type 1, smooth attachment to the triquetrum only; type 2, attachment to the triquetrum and fifth metacarpal bone; type 3, wide attachment on the articular surface of the triquetrum, including the lunotriquetral ligament.

[‡] Attachment types are based on the criteria used by Hogikyan and Louis (9): type 1, small thin structure and focal attachment; type 2, thick structure and focal attachment; type 3, thick structure and broad attachment to between one-third and one-quarter of the triquetrum; type 4, broad attachment covering the entire triquetrum.

Discussion

Taleisnik (5) and Bowers (6) described the UMH as a separable structure extending from the dorsoulnar aspect of the distal radius to the volar-ulnar aspect of the triquetrum. In a purely anatomic study, Ishii et al (7) did not find such a structure; rather, they defined the UMH as the "tissue that is between (and integrated on its periphery) the ulnar aspect of the superficial ligament and the ulnar capsule." These investigators also described three anatomic variations of the UMH with respect to the prestyloid recess that had not been addressed previously. Depending on the shape of the entrance to the prestyloid recess, they classified the opening as narrow, wide, or absent (7). Nishikawa and Toh (8) demonstrated the distal site of attachment of the UMH in 87 embalmed cadavers without using imaging correlation. All UMHs were attached smoothly to the triquetrum. Ninety percent of the UMH specimens were attached to the triquetrum and the fifth metacarpal bone, and 10% were attached widely on the articular surface of the triquetrum, including the lunotriquetral ligament, either partly or completely obscuring the articular surface of the triquetrum.

Hogikyan and Louis (9) subdivided the patterns of distal attachment of the UMH into four groups: pattern 1, a small, thin structure and focal attachment (28%); pattern 2, a thick structure and focal attachment (39%); pattern 3, a thick structure and broad attachment between one-third and one-quarter of the triquetrum (28%); and pattern 4, a broad attachment covering the entire triquetrum (5%). Ono et al (10) reported the presence of a developmental septum that connected the lunotriquetral ligament and the TFC complex in seven of 870 joints, leading to bicompartmentalization of the radiocarpal joint.

Subsequent to these investigations, the anatomic features of the UMH and the relations of the UMH to the anatomic structures on the ulnar side of the wrist were mentioned only infrequently in published studies (11–13). To our knowledge, the findings of Nishikawa and Toh (8), Hogikyan and Louis (9), and Ono et al (10) had never been addressed in a correlative anatomic and MR imaging study.

Most articles have been focused on the radial and central aspects of the TFC complex, and before our current investigation, the anatomic features of the UMH had not been described on MR images by using gross anatomy and histologic examination findings as the reference standard.

In the present study, we further defined the anatomic features, described the imaging characteristics of the different components of the UMH, and visualized the anatomic variants by using MR imaging. Our imaging findings confirm previously published data derived from purely anatomic studies. Knowledge of the anatomic variants is also crucial to the evaluation of the normal anatomy and probably to pathologic changes.

The precise position of the wrist at the time of the examination had a great influence on the imaging characteristics of the UMH. In clinical practice, the wrist is typically imaged in the neutral position. The addition of a coronal sequence performed with the wrist in maximal radial deviation appears to be helpful for evaluating the styloid component of the UMH, the prestyloid recess, and the relationship of the UMH to the ECU tendon sheath and ulnar collateral ligament. In this limited series, we found no benefit to imaging the wrist in maximal ulnar deviation. Theoretically, however, using this position might help in the assessment of the radial side of the radiocarpal joint. No single imaging plane was optimal for the visualization of all components of the UMH, although the most information was derived from observation of the coronal images.

As previously reported by Theumann et al (18), we found no distinct ulnar collateral ligament with MR imaging. Instead, the collateral component of the UMH, the ECU tendon sheath, and the joint capsule were fused indistinguishably, forming what appeared to be a thick ligamentous stabilizer. This finding suggests that the term *ulnar collateral ligament complex* may be more appropriate for describing this composite structure.

At histologic examination, in accordance with the observations of Benjamin et al (19) and Nakamura et al (4), the UMH was composed of fatty, highly vascular dense irregular connective tis-

Figure 10

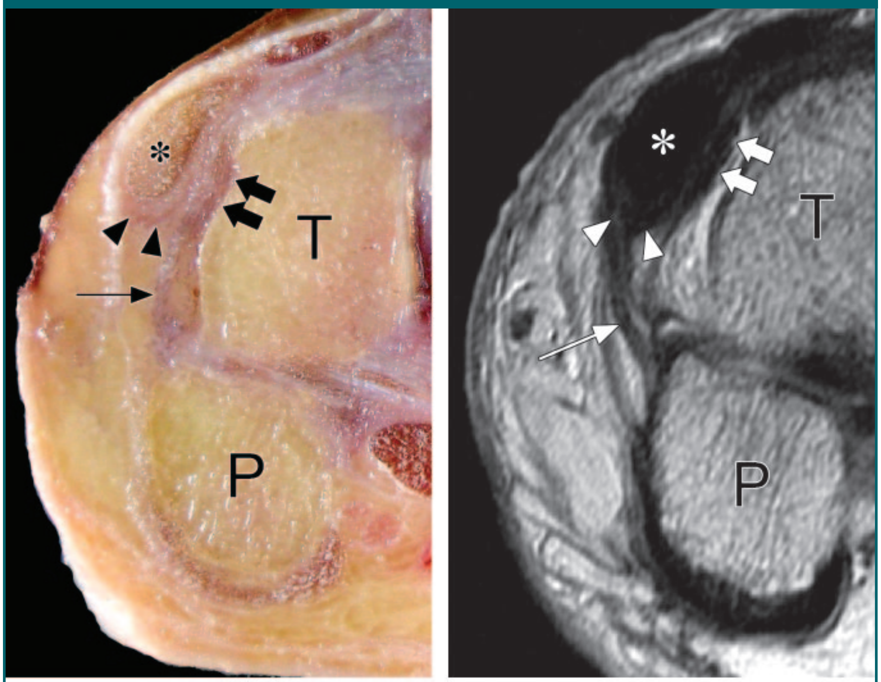

a. b.

Figure 10: **(a)** Gross anatomic section and **(b)** corresponding intermediate-weighted MR image show anatomic features of the distal insertion of the UMH in the transverse plane at the level of the pisotriquetral joint. The fibers at the main insertion into the ulnar aspect of the triquetrum (*T*, thick arrows) are recognized between the triquetrum and the ECU tendon (∗). Some fibers extend further distally (arrowheads) to the base of the ulnar aspect of the hamate bone and the fifth metacarpal bone and are volar to the ECU tendon. In addition, some fibers attach to the ulnar aspect of the pisiform *(P)*, forming the dorsal capsular ligament of the pisotriquetral joint (thin arrow).

sue and densely packed collagen fibers. This composition led to the heterogeneous signal on MR images.

There were some limitations of our study. The number of specimens included was rather small, and the specimen donors were generally older in age at death. Degenerative changes to the UMH could have affected the evaluation of this region. Furthermore, histologic analysis was restricted to five specimens. The clinical implications of these findings are uncertain because we do not yet have examples of lesions of the UMH complex. In conclusion, the anatomy of the UMH is complex. For assessment of the UMH and ulnar side of the TFC complex, coronal MR arthrography with the wrist in neutral position or radial deviation may be superior to conventional MR imaging.

References

1. Lewis OJ, Hamshere RJ, Bucknill TM. The anatomy of the wrist joint. J Anat 1970;106:539–552.
2. Garcia-Elias M. Soft-tissue anatomy and relationships about the distal ulna. Hand Clin 1998;14:165–176.
3. Nakamura T, Makita A. The proximal ligamentous component of the triangular fibrocartilage complex. J Hand Surg Br 2000;25:479–486.
4. Nakamura T, Takayama S, Horiuchi Y, Yabe Y. Origins and insertions of the triangular fibrocartilage complex: a histological study. J Hand Surg Br 2001;26:446–454.
5. Taleisnik J. The ligaments of the wrist. J Hand Surg Am 1976;1:110–118.
6. Bowers WH. The distal radioulnar joint. In: Green DP, ed. Operative hand surgery. Vol 1. 3rd ed. New York, NY: Churchill Livingstone, 1993; 973–1019.
7. Ishii S, Palmer AK, Werner FW, Short WH, Fortino MD. An anatomic study of the ligamentous structure of the triangular fibrocartilage complex. J Hand Surg Am 1998;23:977–985.
8. Nishikawa S, Toh S. Anatomical study of the carpal attachment of the triangular fibrocartilage complex. J Bone Joint Surg Br 2002;84:1062–1065.
9. Hogikyan JV, Louis DS. Embryologic development and variations in the anatomy of the ulnocarpal ligamentous complex. J Hand Surg Am 1992;17:719–723.
10. Ono H, Gilula LA, Marzke MW, Obermann WR. Bicompartmentalization of the radiocarpal joint. J Hand Surg Am 1996;21:788–793.
11. Zlatkin MB, Rosner J. MR imaging of ligaments and triangular fibrocartilage complex of the wrist. Magn Reson Imaging Clin N Am 2004;12:301–331, vi–vii.
12. Totterman SM, Miller RJ. Triangular fibrocartilage complex: normal appearance on coronal three-dimensional gradient-recalled-echo MR images. Radiology 1995;195:521–527.
13. Kauer JM. Functional anatomy of the wrist. Clin Orthop Relat Res 1980;149:9–20.
14. Nakamura T, Yabe Y, Horiuchi Y. Functional anatomy of the triangular fibrocartilage complex. J Hand Surg Br 1996;21:581–586.
15. Nishikawa S, Toh S, Miura H, Arai K. The carpal detachment injury of the triangular fibrocartilage complex. J Hand Surg Br 2002;27:86–89.
16. Palmer AK. Triangular fibrocartilage complex lesions: a classification. J Hand Surg Am 1989;14:594–606.
17. Theumann NH, Pfirrmann CWA, Chung CB, Antonio GE, Trudell DJ, Resnick D. Pisotriquetral joint: assessment with MR imaging and MR arthrography. Radiology 2002;222:763–770.
18. Theumann NH, Pfirrmann CWA, Antonio GE, et al. Extrinsic carpal ligaments: normal MR arthrographic appearance in cadavers. Radiology 2003;226:171–179.
19. Benjamin M, Evans EJ, Pemberton DJ. Histological studies on the triangular fibrocartilage complex of the wrist. J Anat 1990;172:59–67.